Development and Mechanical Design of a Tricycle

Carlos Eduardo Freitas Pereira
carlos.e.f.pereira@tecnico.ulisboa.pt

Instituto Superior Técnico, Universidade de Lisboa, Portugal

June 2018

ABSTRACT

In this paper we intend to provide an overview of the development of an electric tricycle, in collaboration with the company ARSPLUS, Lda. With this purpose, the chassis will be designed considering the average anthropometric measures of the human being as well as some consumers' wants and needs.

Considering the electric motor chosen and based on some considerations about the force created by the human being, the load situation at the start-up will be estimated. We will also analyze the effects caused to the structure due to road irregularities and due to a horizontal impact on the tricycle. To study the structural response of the frame for the two materials analyzed (Reynolds 531 and aluminum alloy 6061 – T6), the Finite Element Method will be used. The safety factor of the project will also be estimated using the Pugsley's Method and the design criteria selected will be the Maximum Allowable Stress criteria.

Finally, a modal analysis will be performed to find the natural frequencies of the frame and the results obtained will be compared with the excitations from the road and the rotation of the wheels and engine. The objective of this analysis is to verify whether resonance exists or not in the chassis.

To design electric tricycle's, the CAD software *SolidWorks 2016* was used and to elaborate the structural and modal analysis, the CAE software used was the *Ansys Workbench 16.0*.

KEYWORDS: Chassis, Finite Element Method, Structural Analysis, Modal Analysis, CAD, CAE.

1. INTRODUCTION

1.1. MOTIVATION

In recent years, awareness and concern about the problems created to the environment by the excessive emissions of carbon dioxide into the atmosphere increased significantly, so research and development of alternative and eco-friendly vehicles has been constant [1].

1.2. HISTORICAL BACKGROUND

In 1680, Stephan Farffler, a German watchmaker with motor disabilities in the lower limbs, invented the first tricycle. Due to his physical condition, the propulsion mechanism that he used were pedals operated by his hands, ensuring that way his mobility [2]. In 1789, two French inventors developed the first pedal-operated tricycle and gave this mechanism the name "tricycle" [2].

1.3. LAYOUT CONFIGURATIONS

A tricycle is a three-wheeled vehicle so, the wheels' layout can fall into one of two possible configurations. The first, and most common, would be the Delta configuration – two rear wheels and one front wheel. The second possibility would be the Tadpole configuration with just one rear wheel and two front wheels.

1.4. DRIVING POSITIONS

Concerning the driving positions, there are two positions that are generally adopted.

Firstly, there is the Upright position, which is a more vertical and right position where the seat is slightly behind the pedals' axis. There is also the Recumbent position, which is a reclined position, where the cyclist can exert a force with his back on the seat and that allows him to increase his pedaling power [3].

1.5. OBJECTIVES

The main objectives of this work are:

• Study the most used materials in the bicycle/tricycle frames' construction;

• Design a geometry based on customers' requirements and ensure proper ergonomics;

• Search and select the most suitable components to incorporate into the tricycle;

• Estimate the loads applied to the structure for later analysis and scaling, ensuring that the project's safety factor is verified;

• Carry out a cost estimate for all elements of the electric tricycle.

2. STATE OF THE ART

2.1. FRAME

The frame is a key component in a tricycle, since it is the structure that connects all the components. When designing a frame, the main goal is to minimize its weight, maximize its strength and rigidity while maintaining an elevated level of comfort and reduced costs. For this purpose, the design and specially the materials used are crucial. Currently, the most used materials are steel and aluminum alloys, titanium and composites [4].

2.1.1. DESIGN/GEOMETRY

Nowadays, three types of frames can be used in tricycles and all of them can be applied in vehicles with Delta or Tadpole configurations. There are the step-through frame, the diamond frame and the recumbent frame.

2.1.2. MATERIALS

2.1.2.1. STEEL ALLOYS

The frames manufactured in steel tend to be the most traditional ones, since this is usually the least expensive material among those listed above and it is easy to work with (both in its construction and in its repair). Other advantages of the frames built in this material are their durability and their strength [5].

2.1.2.2. ALUMINUM ALLOYS

Aluminum is widely used in frames due to its lower density, when compared with steel, and to the fact that it usually has a higher strength/weight ratio, which makes it possible to create lighter and equally resistant frames [5].

2.1.2.3. TITANIUM

Titanium is by far the most expensive material among the most commonly used ones. This is because titanium is a material difficult to machine and to weld, so it is necessary to have specialized labor and machines. Regarding the advantages, this material presents a good fatigue resistance and is often used in the most critical components [5], [6].

2.1.2.4. COMPOSITES

Composite materials can also be used in the construction of frames, namely the composites reinforced with carbon fiber and epoxy matrix. These materials are characterized by their high mechanical strength and low density; however, they can become very expensive once they have a very specific manufacturing process [4]. Another disadvantage about composites is that their quality can only be tested after the entire process of transformation is finished [4].

2.2. BATTERIES

An electric vehicle needs to have its own source of electric power, that is, a battery. So, the battery should be considered one of the main components in this type of vehicles and some of the several types of batteries that exist are:

• Lead-acid battery;
• Nickel-cadmium (Ni-Cd) battery;
• Nickel-metal hydride (Ni-MH) battery;
• Lithium-ion (Li) batteries.

2.3. ELECTRIC MOTORS

The electric motor is an essential component in any electrically assisted vehicle, as it actively intervenes in its propulsion. Currently, there are three types of motors that can be used in the tricycles' industry. They are called hub motors, friction-drive motors and mid-drive motors.

2.3.1. HUB MOTORS

These motors are incorporated directly into the wheel's axis and can be installed either on the rear wheel or front wheel, as the motor is independent of the vehicle's transmission.

2.3.2. MID-DRIVE MOTOR

These motors are installed in the crankshaft and have the peculiarity that they can be designed to be directly coupled in any frame or they may require the development of a specific frame that enables the fixation of the electric motor [7].

2.3.3. FRICTION-DRIVE MOTOR

Friction-drive motors are mounted on the top of a wheel and the driver is assisted by the contact between the electric motor and the tire.

2.3.4. MAXIMUM POWER AND SPEED OF THE ELECTRIC MOTOR

According to Portugal's highway code the help given by the motor is only allowed after the start-up. Its effect must be reduced with speed's increase and must be switched-off when the maximum speed is reached or whenever the driver stops pedaling. The maximum power and speed should not overcome 250 Watt and 25 km/h, respectively [1], [8].

2.3.5. PEDELEC (OR PAS)

Based on the European legislation, the movement aid system must be Pedelec or PAS – Pedal assisted system. This system ensures that the driver contributes to the vehicle's movement because the engine only provides power when the rider is pedaling [1], [8].

2.4. GEARS

Currently, two major types of gear systems are used on tricycles and bicycles. These can be classified as external and internal gears. Within external gears, there are single-speed gears and multi-speed gears. There are also vehicles that do not have any type of gear system, so they use a fixed gear mechanism.

2.4.1. FIXED GEARS

The fixed gear system is the simplest and lightest mechanism that can be used. As its name suggests, it is a fixed mechanism, i.e. the pedals are directly connected to the chain. Thus, the driver can never stop pedaling, since, due to the absence of a free wheel, whenever the wheels are moving, the pedals turn.

2.4.2. SINGLE-SPEED GEARS

A vehicle with a single-speed gear mechanism has only a single gear ratio. Thus, this turns out to be the simplest system that allows freewheel, so the driver can stop pedaling while in motion.

2.4.3. MULTI-SPEED GEARS

Multi-speed gears system is like the single-speed gear system; however, it has the advantage of having more gears, which allows the transmission ratio to be adapted to road conditions and to the driver's capability.

2.4.4. INTERNAL GEARS

Internal gears are also a multi-speed system, however, with the variant of being an internal mechanism (all the components are inserted in a "box", protected from impacts, water and other agents that can wear them). Another advantage of this system is the possibility to change gears even with the vehicle immobilized. Regarding disadvantages, this is a complex and expensive system, and, in case of failure, it is often necessary to change the entire mechanism.

2.5. DESIGN CRITERIA

In the present work, the Maximum Allowable Stress criteria was used for sizing the structure [6]. Thus, it is fundamental to define a project's safety factor and this factor must be respected always for the designed frame to be accepted. The Maximum Allowed Stress, σ_{adm}, will be calculated considering the material's Yield Stress, σ_e, and the project's safety factor, n.

$$\sigma_{\mathrm{adm}} = \frac{\sigma_{\mathrm{e}}}{\mathrm{n}} \tag{2.1}$$

3. COMPONENTS SELECTION

To better understand the consumers' needs and wants, an online form (through a *Google* application) was developed. A few questions were asked with the objective of quantifying some design variables and to choose the best components to incorporate into the tricycle.

3.1. ONLINE FORM RESULTS

Based on the responses given, it was possible to understand some of the requirements pointed out by the potential consumers, such as:

- Autonomy: 30 km;
- Where will be used: roads and urban streets;
- Type of route: with ascents and descents;
- Key features: comfort, safety, low price, stability and minimal maintenance.

3.2. MOTOR

To consider the fact that the type of route most answered by the consumers was "with ascents and descents", the mid-drive motor was selected once it is the best one for this purpose. The electric motor chosen was the *Bafang 8Fun 250 Watt* and this motor produces a maximum torque of 80 N.m, weighs 3.8 kg and costs 360€.

3.3. BATTERY

Considering that the most answer obtained in the form was 30 km for the total autonomy of the vehicle, the battery selected should have a 10.4 A.h capacity (at 20 km/h average speed). The chosen battery was the *Bottle Samsung cells 10.4 A.h*. The cost is 220€ and weighs 2.6 kg.

3.4. GEAR

It was important to choose a gear mechanism that would properly assist the cyclist in climbs and that had minimal maintenance. Considering that, the system chosen was the internal gear and the model selected was the *Sturmey Archer TS-RC3* (a proper component for tricycles). The cost is about 140€ and it weighs 1.36 kg.

3.5. Seat

Comfort was one of the most selected features in the online form and one of the ways to provide comfort to the consumer while driving is by installing a seat with lumbar support. Considering that, the seat chosen is form the brand *Sunlite* and costs 50€.

4. Maximum speed and loading applied to the frame

4.1. Maximum speed

In this topic the maximum speed attainable will be determined, considering the wheels' size used and the maximum cadence that a common rider can produce. Figure 4.1 shows the position of the several sprockets and Table 4.1 presents the teeth's number, Z, of the sprockets.

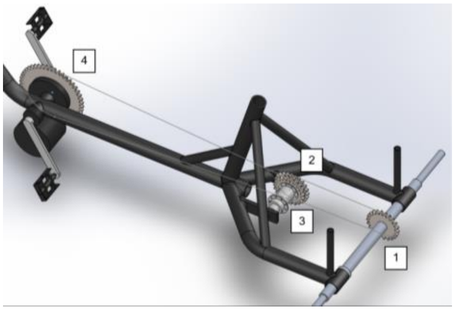

Figure 4.1 - Sprockets' positions on the vehicle.

Table 4.1 - Number of teeth in each sprocket.

	Number of teeth
Z_4	46
Z_3	21
Z_2	24
Z_1	22

Assuming that the diameter of the wheels, D_{wheel}, used in the tricycle is 28'' (≈ 711.2 mm) and the maximum cadence produced by the driver, ω_4, is 90 rpm (≈ 9.43 rad/s) it was possible to conclude that the maximum speed, v_{max}, is 38 km/h. It is important to refer that this value can be greater once these calculations were made neglecting the gravity effects created when, for example, in a descent road. Table 4.2 shows some of the intermediate results obtained.

Table 4.2 - Intermediate results in maximum speed calculation.

ω_1 [rad/s]	29.95	D_1 [mm]	88
ω_2 [rad/s]	27.46	D_2 [mm]	96
ω_3 [rad/s]	20.65	D_3 [mm]	84
ω_4 [rad/s]	9.43	D_4 [mm]	184
ω_{wheel} [rad/s]	29.95	D_{wheel} [mm]	711.2
v_{max} [km/h]	38		

4.2. Loading case 1 – Start-up

To estimate the forces at start-up it was necessary to know the maximum torque of the electric motor, T_{motor}, and what was the maximum torque that a human can produce with his legs, T_{leg}. It was considered that the maximum torque in an electric motor could be reached since the initial moment, that is, from 0 rpm, Figure 4.2.

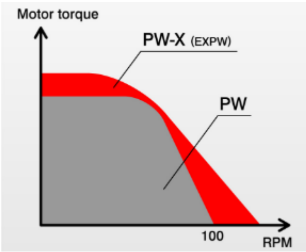

Figure 4.2 – Torque vs. Cadence in a motor [9].

4.2.1. Electric motor's force

As said on the section 3.2, the maximum torque of the *Bafang 8Fun 250 Watt mid-drive motor*, T_{motor}, is 80 N.m. Knowing T_{motor} and knowing the sprocket 4 dimensions, Figure 4.1 and Table 4.2, it is possible to calculate the motor's force, F_{motor}.

$$T_{motor} = F_{motor} \times \frac{D_4}{2} \; ; \; F_{motor} = 870 \; N$$

4.2.2. Pedaling force

To estimate the maximum pedaling force it was necessary to find out what was the maximum torque that a human could produce with his legs, T_{leg}. Considering the experimental data presented in the study made by A. Scott Gardner et all [10], Figure 4.3, it was possible to verify that, in average, a professional cyclist can produce 266 N.m of torque at start-up (0 rpm).

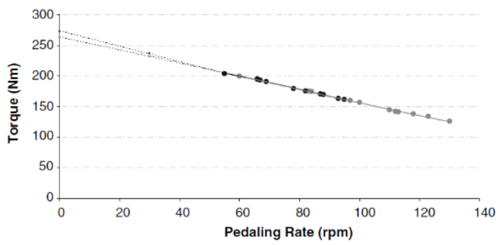

Figure 4.3 - Torque vs. Pedalling rate [10].

This torque was assumed as the maximum torque and, considering that the standard crank length is 170 mm, L_{crank}, the maximum force produced by a human, F_{leg}, was calculated.

$$T_{leg} = F_{leg} \times L_{crank} \; ; \; F_{leg} = 1565 \; N$$

Based on the sprockets' dimensions, Table 4.2, and considering the torque produced by the leg of the driver, T_{leg}, added to the torque produced by the motor, T_{motor}, it was possible to obtain the forces presented in Figure 4.4 and Table 4.3.

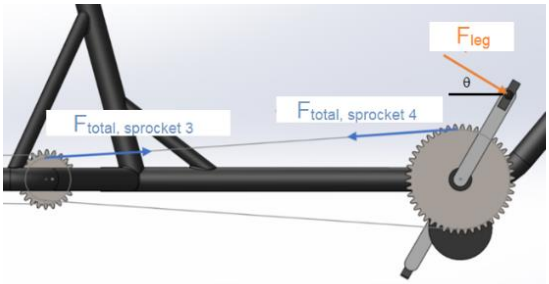

Figure 4.4 – Forces in the sprockets of the front chain (4 and 3).

Table 4.3 - Magnitude of the forces presented in Figure 4.4

$F_{total, sprocket\ 4}$	3761 N
$F_{total, sprocket\ 3}$	

4.2.3. Reaction to the pedaling force

Due to the force created on the pedal by the driver, an equal force, but with opposite direction, will be created (i.e. a reaction). This force, for simplicity, will be applied in the tube of the structure that serves as support for the seat and in this same place will be present the weight of the driver, W_{driver}. The user's leg will be approximated to a bar as shown in Figure 4.5.

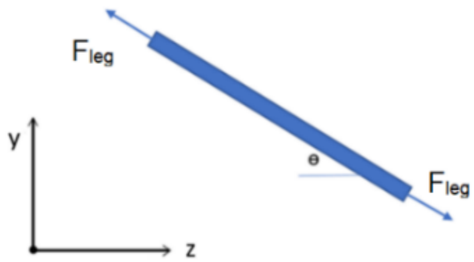

Figure 4.5 - Force and Reaction due to F_{leg}.

Assuming that $\theta \approx 30^o$, due to the frame design, it is possible to calculate the yy and zz component of the F_{leg}.

- $F_{leg, z} = F_{leg} \times \cos(\theta) = 1355$ N
- $F_{leg, y} = F_{leg} \times \sin(\theta) = 782$ N

In Figure 4.6 are represented the forces described previously.

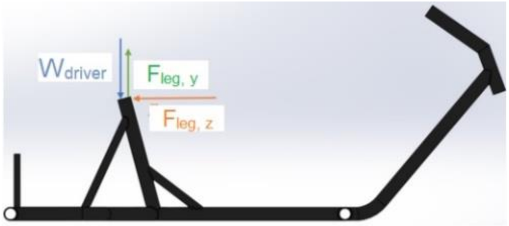

Figure 4.6 - Forces presented in the seat support.

4.2.4. Reactions on the bottom bracket

Due to the force created by the driver's leg, F_{leg}, and to the force in the sprocket 4, several reactions (i.e. torques) appear on the bottom bracket of the frame. Knowing the distances between the tricycle's axis and the sprocket and the pedal, it is possible to calculate the torque due to the $F_{leg, y}$ and the $L_{axis\text{-}pedal}$ (T_z), the torque due to the $F_{leg, z}$ and the $L_{axis\text{-}pedal}$ ($T_{y, 1}$) and the torque due to $F_{total, sprocket\ 4}$ and the $L_{axis\text{-}sprocket}$. Figure 4.7 and Table 4.4 show the results of the reactions on the bottom bracket.Table 4.1

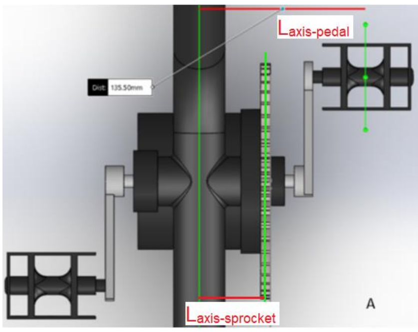

Figure 4.7 – Distance between the axis of the tricycle and the pedal and the sprocket.

Table 4.4 – Distances of the Figure 4.7 and reactions in the bottom bracket

$L_{axis\text{-}pedal}$ [mm]	135.5
$L_{axis\text{-}sprocket}$ [mm]	54
T_z [N.m]	106 (positive)
$T_{y, 1}$ [N.m]	284 (positive)
$T_{y, 2}$ [N.m]	203 (negative)

4.2.5. Sprocket 3 to sprocket 2 (internal gear influence)

Due to the internal gear it will be necessary to account the influence of the gear ratio. The first gear of the system has a gear ratio of 0.75, which is the proper gear for maximum torque. Knowing the total force in the sprocket 3, $F_{total, sprocket\ 3}$, and the sprocket 3's dimension, D_3, it is possible to calculate the torque in the sprocket 3, T_3, and apply the gear ratio to obtain the efforts in the sprocket 2 (T_2 and $F_{total, sprocket\ 2}$). Table 4.5 summarizes the efforts described.

Table 4.5 – Efforts in the sprocket 3 and 2.

$F_{total.\ sprocket\ 3}$ [N]	3761
D_3 [mm]	84
T_3 [N.m]	158
Gear ratio (max. torque)	0.75
T_2 [N]	211
D_2 [mm]	96
$F_{total.\ sprocket\ 2}$ [N]	4388

4.2.6. REACTIONS IN THE MIDDLE SECTION

Figure 4.8 shows the reactions in the tricycle's middle section.

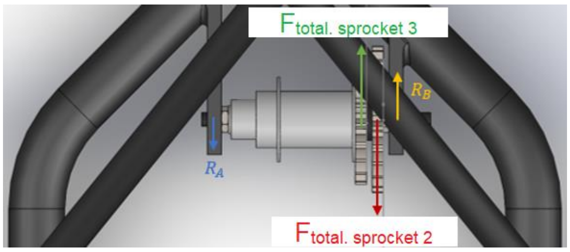

Figure 4.8 – Reactions in the middle section.

Knowing the distances between the point A and the $F_{total,\ sprocket\ 3}$ (L_3), the $F_{total,\ sprocket\ 2}$ (L_2) and the R_B (L_B) it is possible to calculate the reactions in the middle section, Table 4.6.

Table 4.6 – Distances of the Figure 4.8 and reactions in the middle section.

R_A [N]	362
R_B [N]	989
L_3 [mm]	104. 3
L_2 [mm]	116.3
L_B [mm]	119.3

4.2.7. REACTIONS IN THE REAR SECTION

Figure 4.9 shows the reactions in the tricycle's rear section.

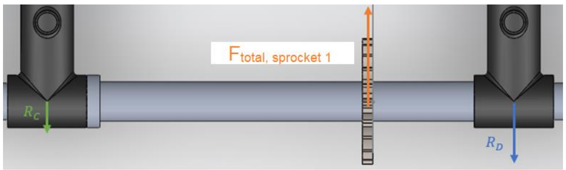

Figure 4.9 - Reactions in the rear section.

Since sprocket 2 and 1 are connected by a chain, $F_{total,\ sprocket\ 2}$ is equal to $F_{total,\ sprocket\ 1}$. Knowing the distances between the point C and the $F_{total,\ sprocket\ 1}$ (L_1) and R_D (L_D), the reactions in the rear section can be calculated, Table 4.7.

Table 4.7 - Distances of the Figure 4.9 and reactions in the rear section.

$F_{total,\ sprocket\ 1}$ [N]	4388
R_C [N]	1375
R_D [N]	3013
L_1 [N]	242.8
L_D [N]	353.6

4.2.8. EFFORTS IN THE HANDLEBAR

The efforts in the handlebar were based on the Figure 4.10 but with some modifications to adapt them to the case of a tricycle.

Figure 4.10 – Efforts in a bicycle's handlebar [11].

Based in the Figure 4.10, it was admitted that the right hand's force, $F_{right\ hand}$, was 159 N and the left hand's force, $F_{left\ hand}$, was 115 N. With the CAD *software* it was possible to make the consideration that these two forces would make 30º with the horizontal axis (due to the vehicle's ergonomics and driver's position).

4.3. LOADING CASE 2 – ROAD IRREGULARITY

The second situation studied was a load that simulated the irregularities in the road, such as road bumps, sidewalk ascents or descents, among others. This case, as shown in Figure 4.11, consists of a 2400 N vertical force, applied to the bicycle seat [11].

Figure 4.11 - "Road irregularities" loading case [11].

4.4. LOADING CASE 3 – HORIZONTAL IMPACT

The third situation analyzed was a horizontal impact in the tricycle. This case, as shown in Figure 4.12, consists of a 1000 N horizontal force applied in the tricycle's fork [12]. For this simulation, the "*Remote Force*" function of the finite element software was used.

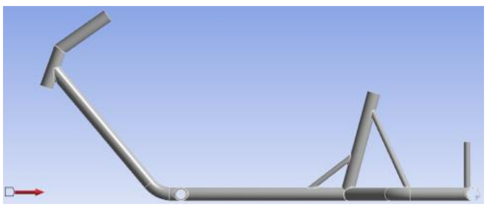

Figure 4.12 – "Horizontal impact" loading case.

4.5. SAFETY FACTOR

The safety factor was estimated using the Pugsley's Method. This method considers various parameters such as properties and quality of the material, accuracy of the analysis performed, the risk to users and the economic impact in case of failure. Using this method, the two components of the safety factor, n_{sx} and n_{sy}, obtained were 1.7 and 1.5, respectively, resulting in a project's safety factor around 2.5.

5. STRUCTURAL ANALYSIS

In this chapter the frame's response will be studied when subjected to the loading cases described in sections 0 to 4.4. The analysis were carried out for the frame built in 6061 – T6 aluminum alloy and for the frame made in Reynolds 531 steel. Table 5.1 shows the materials' properties of the chosen alloys and the allowable stress.

Table 5.1 – Materials' properties [6], [13].

Material	E [GPa]	v	σ_e [MPa]	σ_r [MPa]	σ_{adm} [MPa]
6061 – T6	69	0.33	278	309	109
Reynolds 531	210	0.29	540	770	211

The software used to perform the structural analysis will be the *Ansys Workbench 16.0* and, to guarantee an acceptable level of precision, a convergence analysis will also be carried out.

5.1. LOADING CASE 1 (START-UP) – STRUCTURAL ANALYSIS

In the structural analysis of the first loading case, start-up, the efforts applied to the frame were the ones described in section 4.2. Regarding the constraints applied, vertical movement (yy) was restricted in front and rear supports, to simulate the wheels' influence, and horizontal (zz) movement was restricted in the rear supports, to avoid rigid body movement when a longitudinal effort was applied.

5.1.1. 6061 – T6 ALUMINUM ALLOY

Figure 5.1 shows the different tubes of the tricycle's frame and in the Table 5.2 are their dimensions (external diameter x thickness).

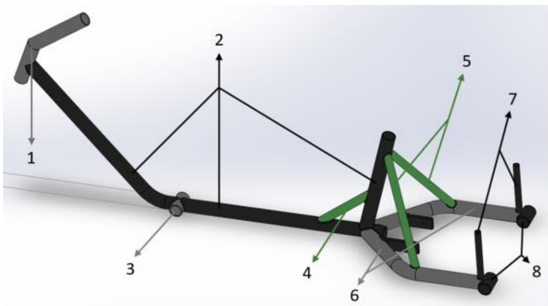

Figure 5.1 - Numeration of the tubes in the frame.

Table 5.2 - Dimensions of the 6061 – T6 aluminium alloy final frame (external diameter x thickness).

Numbers	1, 2, 6 and 8	3	4,5 and 7
Dimensions [mm]	44x3.5	44x5.35	18x1

With the dimensions shown in the Table 5.2, the tricycle's frame weight is 4.1 kg and the results obtained for the "Total Deformation" and "Equivalent Stress" analysis were:

•Max. total deformation: 13.56 mm (Figure 5.2)
•Max. equivalent stress: 107.6 MPa (Figure 5.3)

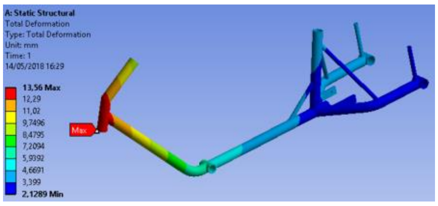

Figure 5.2 – Total Deformation results (6061 – T6, loading case 1).

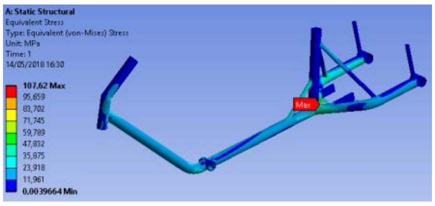

Figure 5.3 – Equivalent stress results (6061 – T6, loading case 1).

The safety factor obtained was 2.55, which is equal to the project's safety factor.

5.1.2. REYNOLDS 531 STEEL

For the situation when the tricycle's frame is made of Reynolds 531 steel, tubes' dimensions presented in Figure 5.1, are shown in Table 5.3.

Table 5.3 - Dimensions of the Reynolds 531 steel final frame (external diameter x thickness).

Numbers	1, 2, 6 and 8	3	4,5 and 7
Dimensions [mm]	45x2.25	45x5.85	20x0.75

With the dimensions shown in Table 5.3, the tricycle's frame weight is 7.3 kg and the results obtained for the "Total Deformation" and "Equivalent Stress" analysis were:

•Max. total deformation: 5.72 mm (Figure 5.4)
•Max. equivalent stress: 211.1 MPa (Figure 5.5)

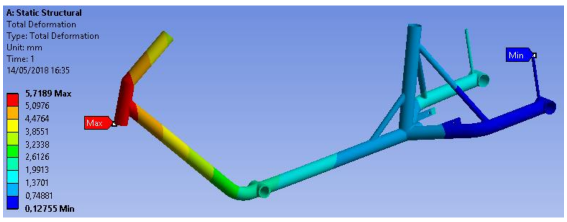

Figure 5.4 – Total Deformation results (Reynolds 531 steel, loading case 1).

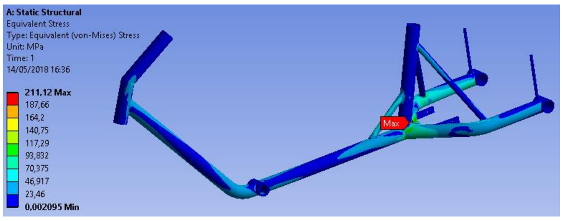

Figure 5.5 – Total Deformation results (Reynolds 531 steel).

The safety factor obtained for this case was 2.56, which is a very close value to the project's safety factor defined in the section 4.5.

5.2. Loading case 2 (road irregularity) – structural analysis

In the structural analysis of the second loading case, road irregularity, the efforts applied to the frame are described in section 4.3 and the frames studied (the one in 6061 – T6 aluminum alloy and the other in Reynolds 531 steel) were the ones obtained in the section 5.1.1 and 5.1.2, respectively. The constraints applied were the same as the ones used in the loading case 1.

5.2.1. 6061 – T6 aluminum alloy

In the case of the structure made in 6061 – T6 aluminum alloy, the results obtained for the "Total Deformation" and "Equivalent Stress" analysis were:

•Max. total deformation: 2.15 mm (Figure 5.6)
•Max. equivalent stress: 66.7 MPa (Figure 5.7)

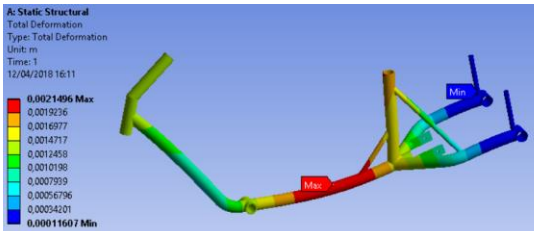

Figure 5.6 – Total Deformation results (6061 – T6, loading case 2).

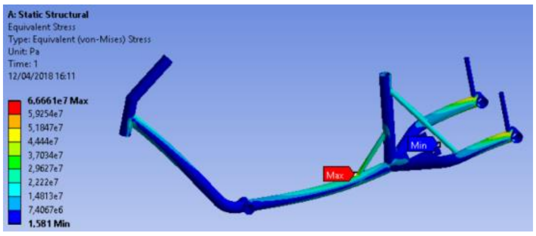

Figure 5.7 – Equivalent stress results (6061 – T6, loading case 2).

The safety factor obtained for this case was 4.2, which is very superior to the value of the project's safety factor defined in the section 4.5.

5.2.2. Reynolds 531 steel

In the structure made in Reynolds 531 steel, the results obtained for the "Total Deformation" and "Equivalent Stress" analysis were:

•Max. total deformation: 1.12 mm (Figure 5.8)
•Max. equivalent stress: 120 MPa (Figure 5.9)

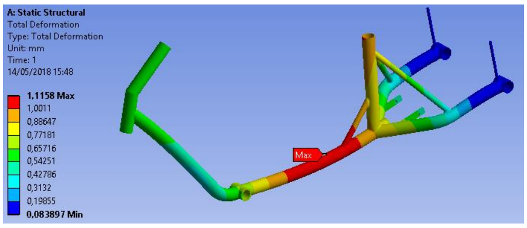

Figure 5.8 – Total Deformation results (Reynolds 531 steel, loading case 2).

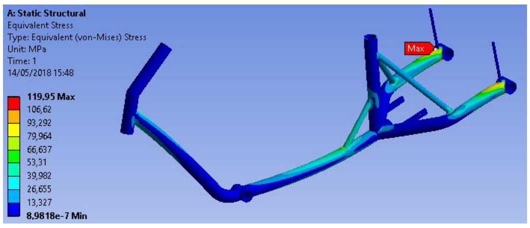

Figure 5.9 – Total Deformation results (Reynolds 531 steel, loading case 2).

The safety factor obtained for this case was 4.5, which is very superior to the value of the project's safety factor defined in the section 4.5.

5.3. Loading case 3 (horizontal impact) – structural analysis

In the structural analysis of the third loading case, road irregularity, the efforts applied to the frame were the ones described in section 4.4 and the frames studied (the one in 6061 – T6 aluminum alloy and the other in Reynolds 531 steel) were the ones obtained in the section 5.1.1 and 5.1.2, respectively.

Regarding the constraints applied on the structure, the option "Displacement" of the finite element software was used. Thus, vertical (yy) and longitudinal (zz) movement were restricted in the rear supports.

5.3.1. 6061 – T6 aluminum alloy

In the case of the structure made in 6061 – T6 aluminum alloy, the results obtained for the "Total Deformation" and "Equivalent Stress" analysis were:

•Max. total deformation: 7.3 mm (Figure 5.10)
•Max. equivalent stress:172.3 MPa(Figure 5.11)

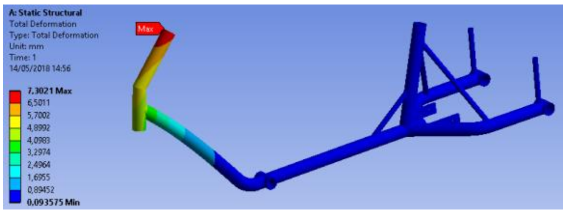

Figure 5.10 – Total Deformation results (6061 – T6, loading case 3).

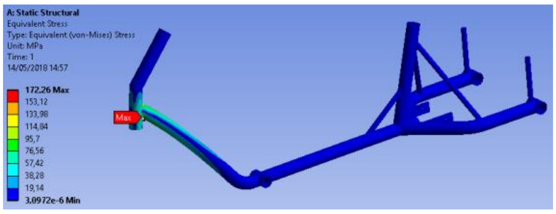

Figure 5.11 – Equivalent stress results (6061 – T6, loading case 3).

The safety factor obtained for this case was 1.6. Despite the fact that the safety factor obtained was inferior to the project's safety factor, this is a critical situation, so, as long as the safety factor is bigger than 1, it is guaranteed that the structure will not collapse.

5.3.2. REYNOLDS 531 STEEL

In the structure made in Reynolds 531 steel, the results obtained for the "Total Deformation" and "Equivalent Stress" analysis were:

•Max. total deformation: 4.1 mm (Figure 5.12)
•Max. equivalent stress:261.7 MPa(Figure 5.13)

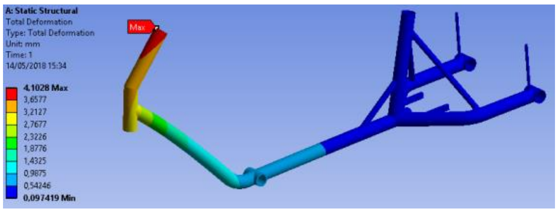

Figure 5.12 – Total Deformation results (Reynolds 531 steel, loading case 3).

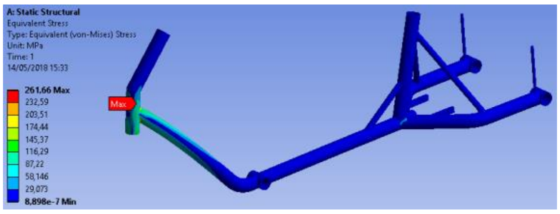

Figure 5.13 – Total Deformation results (Reynolds 531 steel, loading case 3).

The safety factor obtained for this case was 2.06. Despite the fact that the safety factor obtained was inferior to the project's safety factor, this is a critical situation, so, as long as the safety factor is bigger than 1, it is guaranteed that the structure will not collapse.

6. MODAL ANALYSIS

Vibrations often lead to undesired effects, such as higher amplitudes of motion than the ones projected, excitation of resonance frequencies of the structure causing instability situations. The modal analysis is then one of the most used techniques to predict how a structure will react to vibrations and understand what is going to be its response to a dynamic request. In Table 6.1 are presented the vibration modes and natural frequencies of the frame (free-free fixtures).

Table 6.1 – Vibration modes and natural frequencies of the frame.

Vibration modes	Natural frequencies [Hz]	
	Aluminum	Steel
1	52.53	54.84
2	62.14	68.14
3	119.79	128.5
4	149.96	128.57
5	158.35	164.03
6	210.09	215.67
7	289.17	238.69
8	304.22	287.98
9	393.33	300.83
10	429.59	310.89

7. COSTS ESTIMATE

7.1. COST OF THE FRAME

To estimate the frame's cost, the information present in the Table 5.2 and in the Table 5.3 was used and the length of each set of tubes was added and increased by 30% (to prevent some defects or wastes) in order to calculate the price of each one, Table 7.1.

Table 7.1 – Length and price of the tubes presented in Figure 5.1 [14].

	Tube's length [mm]	Tube's length increased [mm]	Price of the steel tubes (€)	Price of the aluminum tubes (€)
1, 2, 6, 8	2550	3315	17.10	18.90
3	68	90	18.30	13.00
4, 5, 7	1078	1400	2.40	2.30

Based on Table 7.1, it is possible to calculate the raw material cost to construct either the aluminum frame or the steel frame. The total price of the aluminum tubes would be 34.20€ and the total price of the steel tubes would be 37.80€. Comparing the cost of each raw material we can conclude that this parameter cannot be used as a differentiating factor.

7.2. COST OF THE OTHER COMPONENTS.

The costs associated with some of the elements to be included in the electric tricycle have already been stated in section 3, i.e. the electric motor, battery, gear system and seat. Table 7.2 summarizes the prices of those components and some others that must be incorporated.

Table 7.2 - Estimative of the several components.

Components	Price
Electric motor	360€
Battery	220€
Gear system	140€
Brakes system	90€
Seat	50€
Seat post and seat clamp	25€
28'' wheels	150€
Handlebar and stem	30€
Fork and rear axis (raw material)	20€
Basket	30€
Total	**1115€**

Considering Table 7.2 the total cost of the various components is 1115€ and, if we estimate that the frame could cost around 450€, the projected electric tricycle would have a base price of approximately 1600€.

8. CONCLUSIONS

In this paper, the main objective was to design an electric tricycle. During the process, it was possible to conclude that a vehicle like this should be faced as a solid alternative to the traditional ones due to its various advantages.

To carry out the structural analyses made to the tricycle's frame we started by estimating the efforts present during the three loading cases analyzed. It was also necessary to define the project's safety factor to determine the maximum allowable stress in the structure.

With the analyses performed it was possible to draw some conclusions about the frame's behavior and, to choose the most appropriate material, a cost estimate analysis was made, however, it was inconclusive. Therefore, it was necessary to account for the material's influence on safety.

Regarding safety, the steel frame offers smaller distortions and it can be designed for infinite life (unlike an aluminum frame). Another advantage of the steel frame is that it is easier to repair. Even though the steel frame weighs more 3 kg than the aluminum frame, it was not given much importance to this since the vehicle's total mass is much bigger (around 30 kg).

9. FUTURE DEVELOPMENTS

As a suggestion for a future work, a fatigue analysis study should be carried out, since this is one of the biggest causes of failure in bicycles and tricycles, so it is extremely important to consider this effect when dimensioning a frame. Finally, to confirm the numerical analyses performed, a prototype could be built to elaborate experimental tests and then compare the results obtained by the two methods.

10. REFERENCES

[1] I. V. McLoughlin *et al.*, "Campus Mobility for the Future: The Electric Bicycle," *J. Transp. Technol.*, vol. 2, pp. 1–12, 2012.

[2] S. Greene, *FREE on THREE: The Wild World of Human Powered Recumbent Tadpole TriCycles*. iUniverse, 2011.

[3] D. G. Wilson, "Understanding Pedal Power," pp. 1–18, 1986.

[4] "A Bicicleta como um Caso de Design Industrial," Faculdade de Engenharia da Universidade do Porto, Tese de Mestrado, 2003.

[5] P. M. T. Ribeiro, "Análise dinâmica de um quadro de bicicleta", Faculdade de Engenharia da Universidade do Porto, Tese de Mestrado, 2013.

[6] A. D. Silva, A. D. Ferreira, M. I. Costa, and S. A. Abreu, "Análise Estrutural do Quadro de uma Bicicleta", Faculdade de Engenharia da Universidade do Porto, Tese de Mestrado, 2014.

[7] A. Matasyan, "Technical analysis and market study of electric bicycles", Universitat Politècnica de Catalunya, Tese de Mestrado, 2015.

[8] N. Sousa, A. E. Gonçalves, and J. Coutinho-Rodrigues, "Pedelec on a Hilly City : a Case Study in Coimbra", *Energy Sustain. Int. Conf. 2017*, pp. 1–7, 2017.

[9] https://global.yamaha-motor.com/business/e-bike-systems/pw-x/drive-unit/ [25-Aug-2017].

[10] A. S. Gardner, J. C. Martin, D. T. Martin, M. Barras, and D. G. Jenkins, "Maximal torque and power-pedaling rate relationships for elite sprint cyclists in laboratory and field tests", *Eur. J. Appl. Physiol.*, vol. 101, pp. 287–292, 2007.

[11] L. Maestrelli and A. Falsini, "Bicycle Frame Optimization By Means of an Advanced Gradient Method Algorithm", pp. 1–16, 2008.

[12] S. S. Quek and G. R. Liu, *Finite Element Method: A Practical Course*, First Edit. Butterworth-Heinemann, 2003.

[13] H. J. Liu, H. Fujii, M. Maeda, and K. Nogi, "Tensile properties and fracture locations of friction-stir-welded joints of 6061-T6 aluminum alloy", *J. Mater. Sci. Lett.*, vol. 22, pp. 1061–1063, 2003.

[14] http://www.custompartnet.com [Accessed: 09-Oct-2017].